

## RESEARCH ARTICLE

# Micelle-crosslinked hydrogels with stretchable, self-healing, and selectively adhesive properties: Random copolymers work as dynamic yet self-sorting domains

Hiroaki Asai<sup>1</sup> | Motoki Shibata<sup>2</sup>  | Mikihiro Takenaka<sup>3,4</sup>  | Shinichi Takata<sup>5</sup> |  
Kosuke Hiroi<sup>5</sup> | Makoto Ouchi<sup>1</sup>  | Takaya Terashima<sup>1</sup> 

<sup>1</sup>Department of Polymer Chemistry, Graduate School of Engineering, Kyoto University, Katsura, Kyoto, Japan

<sup>2</sup>Office of Society-Academia Collaboration for Innovation, Kyoto University, Yoshida-honmachi, Kyoto, Japan

<sup>3</sup>Institute for Chemical Research, Kyoto University, Uji, Kyoto, Japan

<sup>4</sup>RIKEN SPring-8 Center, Sayo-cho, Sayo-gun, Hyogo, Japan

<sup>5</sup>J-PARC Center, Japan Atomic Energy Agency, Tokai, Ibaraki, Japan

## Correspondence

Takaya Terashima, Department of Polymer Chemistry, Graduate School of Engineering, Kyoto University, Katsura, Nishikyo-ku, Kyoto 615-8510, Japan.  
Email: [terashima.takaya.2e@kyoto-u.ac.jp](mailto:terashima.takaya.2e@kyoto-u.ac.jp)

## Funding information

Japan Society for the Promotion of Science KAKENHI, Grant/Award Numbers: JP19K22218, JP20H02787, JP20H05219, JP22H04539; The Ogasawara Foundation for the Promotion of Science & Engineering; Noguchi Institute; Iketani Science and Technology Foundation

## Abstract

The design of crosslinking domains is a vital factor to create functional hydrogels with controlled physical, mechanical, and adhesive properties. This paper demonstrates versatile synthetic systems of micelle-crosslinked hydrogels with highly stretchable, self-healing, and selectively adhesive properties. For this, methacrylate-bearing random copolymer micelles are designed as physical and covalent crosslink domains via the self-assembly of amphiphilic random copolymers carrying hydrophilic poly(ethylene glycol) (PEG), hydrophobic butyl or dodecyl groups, and methacrylate-terminal PEG in water. The size, aggregation number, and pendant methacrylate number of the micelles are controlled by the composition and degree of polymerization. Hydrogels are efficiently obtained from the free radical polymerization of hydrophilic monomers such as PEG acrylate and acrylamide in the presence of the micelle crosslinkers in water. Owing to the dynamic yet selective chain exchange properties of the micelle domains, the hydrogels are highly stretchable up to over 1000% and show self-healing and selectively adhesive properties. The self-healing of hydrogels is promoted upon heating due to the fast chain exchange of the micelle domains, whereas hydrogels consisting of micelles with different alkyl groups are never adhesive because of their self-sorting properties.

## KEYWORDS

adhesion, hydrogel, random copolymer micelle, self-assembly, self-healing, self-sorting

## 1 | INTRODUCTION

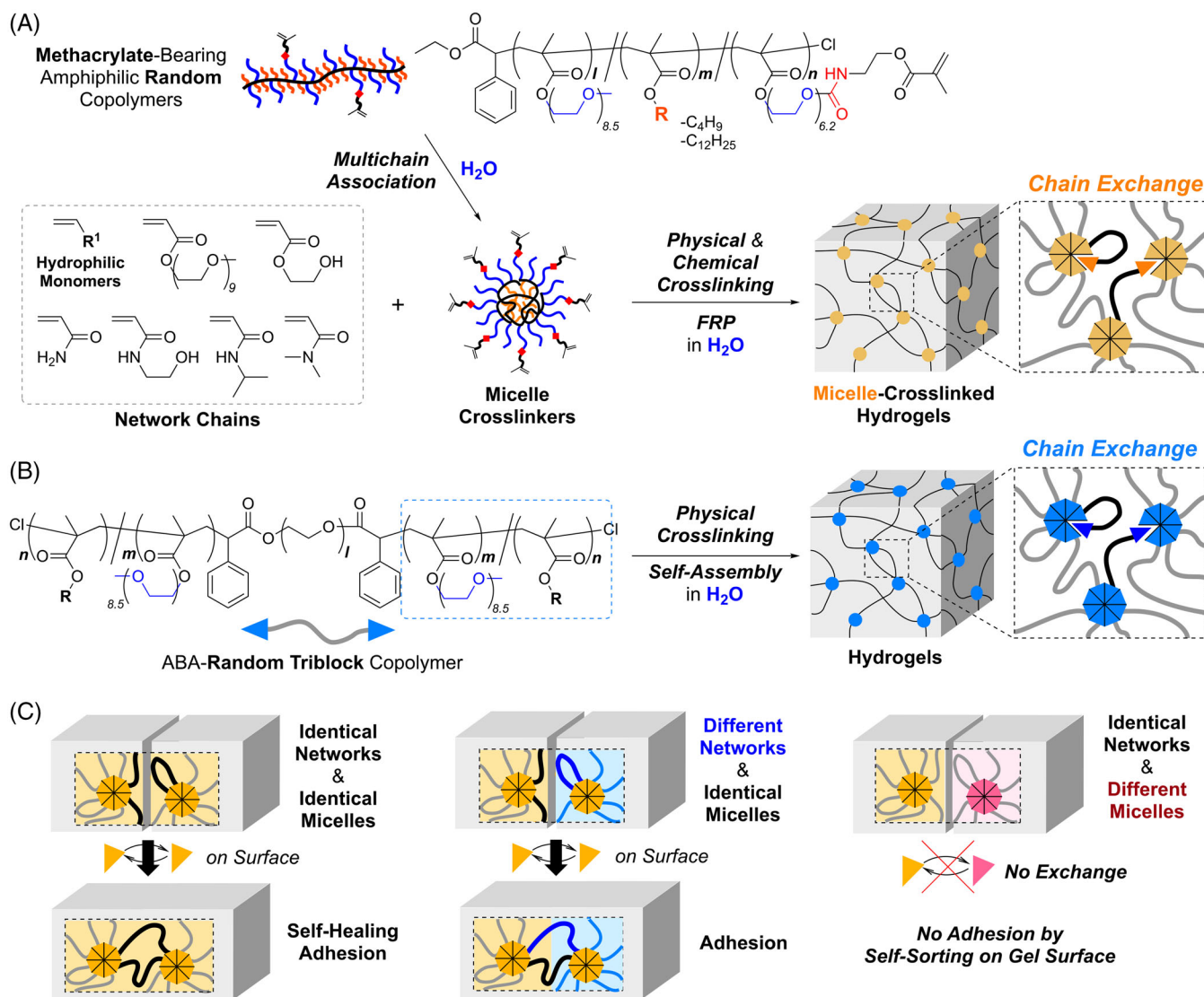
Hydrogels are soft materials consisting of three-dimensional networks swelled by water. Owing to the design versatility, tunable physical properties, and biocompatibility, hydrogels are utilized in various research fields and are typically effective as biomaterials for tissue engineering, drug delivery, and many others.<sup>[1–5]</sup> Many types of gelation systems have been developed to create network polymer materials and hydrogels with excellent mechanical properties and intriguing functions such as self-healing properties and shape memory effects. The physical properties and functions depend on the structure, density, and dynamic properties of crosslinking units, in addition to the design of network chains. In general, crosslinking of network chains involves covalent bond

formation (chemical crosslinking) or physical association and entanglement via hydrophobic effects, hydrogen-bonding or ionic interactions, and complex formation. Importantly, dynamic crosslinking via physical association or mobile and exchangeable units serve as sacrificial bonding or resilient and reversible connection of network polymer chains when gel materials are strained by tensile or shear stress.<sup>[6–8]</sup> Therefore, such dynamic crosslinking systems often lead to highly stretchable and excellent mechanical properties and adhesive properties, as realized by double network gels,<sup>[9,10]</sup> interpenetrating gels,<sup>[11]</sup> slide-ring gels,<sup>[12,13]</sup> hydrogels with supramolecular recognition,<sup>[14,15]</sup> and micelle-crosslinked gels.<sup>[16–29]</sup>

Among them, polymer micelles bearing multifunctional units such as post-reacting vinyl groups are promising

This is an open access article under the terms of the [Creative Commons Attribution](https://creativecommons.org/licenses/by/4.0/) License, which permits use, distribution and reproduction in any medium, provided the original work is properly cited.

© 2023 The Authors. *Aggregate* published by SCUT, AIEI, and John Wiley & Sons Australia, Ltd.



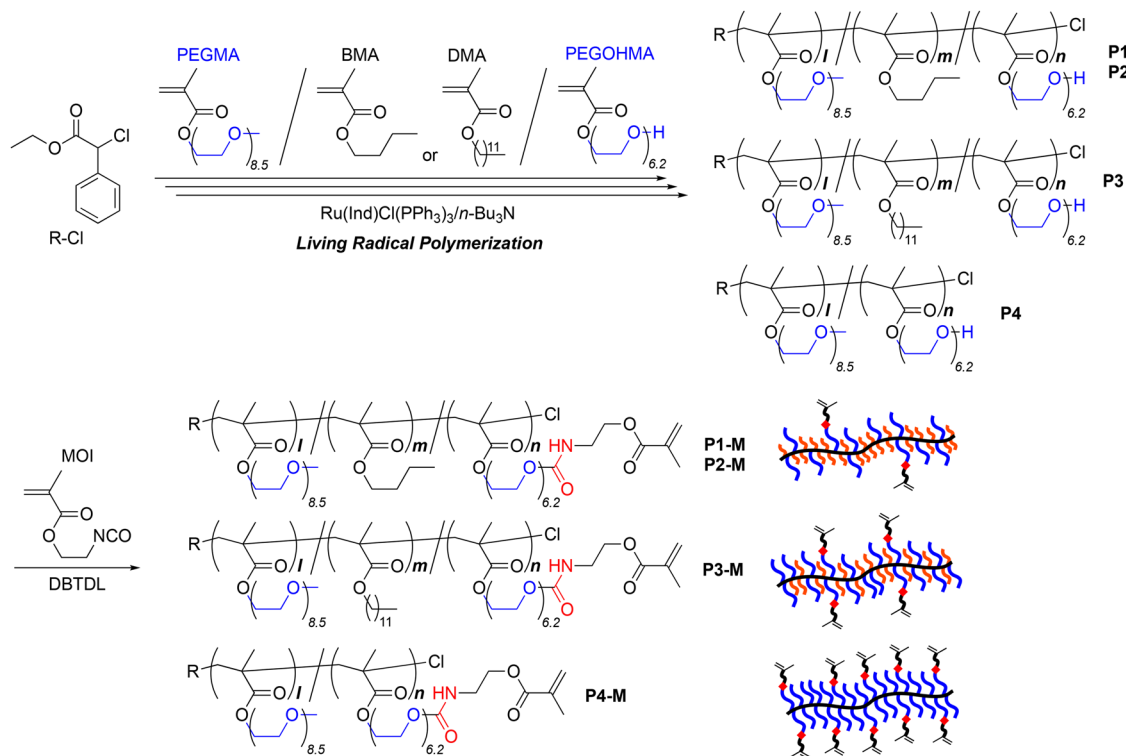
**SCHEME 1** (A) Hydrogels prepared via free radical polymerization of hydrophilic monomers with methacrylate-bearing amphiphilic random copolymer micelles as physical and chemical crosslinking points. (B) Hydrogels via the self-assembly of ABA-random triblock copolymers. (C) Self-healing and adhesive properties of micelle-crosslinked hydrogels

as physically and/or chemically crosslinked domains for hydrogels.<sup>[22–29]</sup> For example, pluronic surfactants [poly(ethylene oxide)-poly(propylene oxide)-poly(ethylene oxide), PEO-PPO-PEO],<sup>[22–25]</sup> macromolecular surfactants,<sup>[26,27]</sup> and amphiphilic block copolymers<sup>[28,29]</sup> have been employed for micelle crosslinking agents. Even after radical crosslinking reactions using hydrophilic monomers such as acrylamide (AAM), their polymer micelles bearing multiple vinyl groups reversibly and dynamically induce physical association by hydrophobic effects and thus offer energy dissipation in hydrogels, leading to highly stretchable and excellent mechanical properties.

Recently, we have developed controlled self-assembly systems of amphiphilic random copolymers with hydrophilic poly(ethylene glycol) (PEG) and hydrophobic alkyl groups as side chains to create size-controlled but small micelles in water.<sup>[30–35]</sup> Uniquely, the random copolymers induce chain-folding via the association of the hydrophobic alkyl groups in water and form folded micelles whose size (~10 nm) is much smaller than that of corresponding block copolymer micelles.

The micelle size and aggregation number can precisely be controlled by their degree of polymerization (DP), copolymer composition, and side-chain structures. More importantly, the random copolymer micelles show dynamic self-sorting via chain exchange and self-recognition in water: The copolymer chains are exchanged between micelles with identical composition and hydrophobic groups, whereas copolymer chains consisting of different compositions and/or alkyl pendants are not associated each other and thus give discrete micelles of their respective copolymers.

Focusing on the dynamic self-assembly and self-sorting behavior, we previously designed amphiphilic ABA-triblock copolymers comprising the amphiphilic random copolymer A segments and a hydrophilic PEG chain B segment to produce hydrogels (Scheme 1B).<sup>[32]</sup> The random copolymer A segments induced self-assembly to form micelles as physical crosslink domains. The hydrogels showed self-healing properties via chain exchange between the crosslink domains but never adhered to hydrogels consisting of different micelles due to the self-sorting behavior. Thus, we found that random



**SCHEME 2** Synthesis of methacrylate-bearing amphiphilic random copolymers (**P1-M**, **P2-M**, **P3-M**, and **P4-M**) via living radical polymerization of poly(ethylene glycol) methyl ether methacrylate (PEGMA), butyl methacrylate (BMA) or dodecyl methacrylate (DMA), and PEG methacrylate with a hydroxy group (PEGOHMA) and post-functionalization of the copolymers with an isocyanate-bearing methacrylate (MOI)

copolymer micelles were effective as crosslinked domains for hydrogels with self-healing but selectively adhesive properties.

Given these backgrounds, we herein report a versatile strategy to design micelle-crosslinked hydrogels with highly stretchable, self-healing, and selectively adhesive properties (Scheme 1A). The objectives of this paper are to establish a novel strategy to produce hydrogels with micelle-crosslinked domains and investigate their physical and adhesive properties. It should be noted that the synthetic approaches enable us to combine various hydrophilic polymer networks and micelle-crosslinkers via simple free radical polymerization (FRP) of hydrophilic vinyl monomers in the presence of multifunctional random copolymer micelles in water. Thus, this strategy is more efficient and easier than the previous gelation systems with the amphiphilic ABA-triblock copolymers in designing hydrogels: the previous system required the preparation of various macroinitiators (B segments) to modify network polymer chains for targeted physical properties and functions. Additionally, the micelles in this novel gelation system work as not only physical but also chemical crosslinking domains to afford the diverse tuning of the physical properties (mechanical, rheological, stretchable properties, etc.).

For this, we designed amphiphilic random copolymers bearing hydrophilic PEG, hydrophobic alkyl (butyl or dodecyl) groups, and methacrylate-capped PEG as side chains to produce folded multichain micelles as crosslinkers in water. The size and aggregation number of the micelles were controlled by the DP, alkyl groups, and composition, and thus the number of methacrylate units (for crosslinking) per a single micelle domain was also controlled. Micelle-crosslinked hydrogels were obtained from the FRP of hydrophilic

monomers in the presence of the micelle crosslinkers. The rheological, stretching, self-healing, and adhesive properties of their hydrogels were investigated systematically by varying the micelle concentration and structures and hydrophilic monomers. Owing to the dynamic self-assembly and self-sorting properties of the micelle crosslinkers, the hydrogels showed highly stretchable, self-healing, but selectively adhesive properties (Scheme 1C).

## 2 | RESULTS AND DISCUSSION

### 2.1 | Design and synthesis of methacrylate-bearing amphiphilic random copolymers

Methacrylate-carrying amphiphilic random copolymers (**P1-M**–**P4-M**) were designed as crosslinking domains for hydrogels. **P1-M**–**P4-M** were synthesized by living radical copolymerization of hydrophilic PEG methyl ether methacrylate (PEGMA: average number of oxyethylene units = 8.5), hydrophobic butyl or dodecyl methacrylate (BMA or DMA), and PEG methacrylate with a hydroxy group (PEGOHMA: average number of oxyethylene units = 6.2), followed by the post-functionalization of the resulting random copolymer precursors (**P1**–**P4**) with 2-methacryloyloxyethyl isocyanate (MOI) (Scheme 2). The methacrylate units introduced into the PEGOHMA terminals are expected to exist in the outer layers of their micelles and polymers in water and thus undergo efficient crosslinking. According to our previous investigations,<sup>[30,31]</sup> the content of BMA and DMA was set to 70 mol% and 50 mol%, respectively, to produce size-controlled micelles in water. **P1-M** and **P2-M**, both of which

TABLE 1 Characterization of amphiphilic random copolymers

Polymer <sup>a</sup>	RMA <sup>a</sup>	RMA <sup>b</sup> (mol%)	DP <sup>b</sup>	<i>l/m/n</i> <sup>b</sup> (NMR)	<i>M<sub>n</sub></i> <sup>c</sup> (SEC)	<i>M<sub>w</sub>/M<sub>n</sub></i> <sup>c</sup> (SEC)	<i>M<sub>w</sub></i> <sup>d</sup> (calcd)	<i>M<sub>n</sub></i> <sup>b</sup> (NMR)	<i>M<sub>w,DMF</sub></i> <sup>e</sup> (MALLS)	<i>M<sub>w,H<sub>2</sub>O</sub></i> <sup>e</sup> (MALLS)	<i>N<sub>agg</sub></i> <sup>f</sup>
<b>P1</b>	BMA	71	106	29/75/2	26,400	1.18	29,700	25,200	35,500	289,000	8.2
<b>P1-M</b>					26,700	1.17	29,800	25,500	35,600	340,000	9.6
<b>P2</b>	BMA	72	113	21/81/11	28,600	1.18	30,100	25,500	38,000	337,000	8.9
<b>P2-M</b>					30,500	1.17	31,800	27,200	44,700	–	–
<b>P3</b>	DMA	53	103	44/55/4	21,600	1.33	48,400	36,400	53,000	435,000	8.2
<b>P3-M</b>					22,600	1.32	48,700	36,900	56,100	501,000	8.9
<b>P4</b>	–	0	56	35/0/21	27,700	1.26	30,500	24,200	39,000	46,100	1.2
<b>P4-M</b>					30,000	1.23	36,900	27,400	44,600	52,800	1.2

<sup>a</sup>**P1**, **P2**, **P3**, and **P4** were synthesized by living radical copolymerization of poly(ethylene glycol) methyl ether methacrylate (PEGMA), butyl methacrylate (BMA) or dodecyl methacrylate (DMA), and poly(ethylene glycol) methacrylate (PEGOHMA). **P1-M**, **P2-M**, **P3-M**, and **P4-M** were synthesized by the quantitative functionalization of **P1**, **P2**, **P3**, and **P4** with 2-methacryloyloxyethyl isocyanate (MOI).

<sup>b</sup>BMA or DMA content, total degree of polymerization (DP), and the number of PEGMA (*l*), BMA or DMA (*m*), and PEGOHMA (*n*), and number-average molecular weight (*M<sub>n</sub>*) of the copolymers determined by <sup>1</sup>H NMR.

<sup>c</sup>Number-average molecular weight (*M<sub>n</sub>*) and molecular weight distribution (*M<sub>w</sub>/M<sub>n</sub>*) of the copolymers determined by SEC in DMF (10 mM LiBr) with PMMA standard calibration.

<sup>d</sup>Weight-average molecular weight of the copolymers calculated with *M<sub>n</sub>* (NMR) and *M<sub>w</sub>/M<sub>n</sub>* (SEC): *M<sub>w</sub>* (calcd) = *M<sub>n</sub>* (NMR) × *M<sub>w</sub>/M<sub>n</sub>* (SEC).

<sup>e</sup>Absolute weight-average molecular weight of the polymers (*M<sub>w</sub>*) determined by SEC-MALLS in DMF (10 mM LiBr) or H<sub>2</sub>O (100 mM NaCl).

<sup>f</sup>Aggregation number of the copolymers and micelles in H<sub>2</sub>O: *N<sub>agg</sub>* = *M<sub>w,H<sub>2</sub>O</sub>* (MALLS)/*M<sub>w,DMF</sub>* (MALLS).

contain 70 mol% BMA, have 2 and 11 pendant methacrylate units per chain, respectively. **P3-M** with 50 mol% DMA has 4 pendant methacrylate units per chain. **P4-M** without hydrophobic monomers serves just as a covalent crosslink domain in water, into which 21 methacrylate units were introduced to set the number close to that of a single **P1-M** micelle in water.

**P1–P4** were prepared by the copolymerization of PEGMA, BMA or DMA, and PEGOHMA with a chloride initiator (ethyl 2-chloro-2-phenylacetate) and a ruthenium catalyst [Ru(Ind)Cl(PPh<sub>3</sub>)<sub>2</sub>/*n*-Bu<sub>3</sub>N] in toluene at 80°C. PEGMA, BMA or DMA, and PEGOHMA were smoothly consumed to give well-controlled random copolymers, regardless of their pendants and composition (*M<sub>n</sub>* = 21,600–28,600, *M<sub>w</sub>/M<sub>n</sub>* = 1.18–1.33 by size exclusion chromatography (SEC) in DMF with PMMA standard calibration, Table 1 and Figure S1). PEGMA (PEGOHMA) and BMA or DMA were simultaneously consumed at the same speed during copolymerization, meaning that PEG and alkyl groups were randomly distributed along each polymer chain. All the products were analyzed by <sup>1</sup>H nuclear magnetic resonance (<sup>1</sup>H NMR) spectroscopy to determine the composition, DP, and the number of monomer units (PEGMA/BMA or DMA/PEGOHMA = *l/m/n*) (Table 1, Figure 1, and Figure S2). The *l/m/n* values, estimated from the area ratio of their monomer units to that of the initiator Ph group, were close to those calculated from the feed ratio of their respective monomers to the initiator and their monomer conversion. The number-average molecular weight of the copolymers (*M<sub>n</sub>*) was determined to be 24,200–36,400 by <sup>1</sup>H NMR.

**P1-M–P4-M** were obtained by mixing **P1–P4** and MOI with dibutyltin dilaurate as a catalyst in dichloromethane at 25°C. As confirmed by <sup>1</sup>H NMR, the hydroxyl groups of **P1–P4** completely disappeared, and the methacrylate units were introduced quantitatively (Figure 1 and Figure S3). **P1-M–P4-M** had molecular weight close to their corresponding precursors (*M<sub>n</sub>* = 22,600–30,500, *M<sub>w</sub>/M<sub>n</sub>* = 1.17–1.32 by SEC in DMF with PMMA standard calibration, Figure 1 and Table 1). The number-average molecular weight of **P1-M–**

**P4-M** was determined to be 25,500–36,900 by <sup>1</sup>H NMR. Additionally, **P1-M–P4-M** and their precursors were analyzed by SEC coupled with multi-angle laser light scattering (SEC-MALLS) in DMF to determine absolute weight-average molecular weight (*M<sub>w,DMF</sub>*) for the calculation of the aggregation number of their micelles in water (Table 1).

## 2.2 | Self-Assembly of copolymers into micelles for crosslinking domains in water

Self-assembly of amphiphilic random copolymers (**P1-M–P4-M**, **P1–P4**) into micelles in water was examined by SEC-MALLS. All the copolymers were easily dissolved in water. The micelles were prepared via the following processes: The copolymers were mixed with pure water in vials at 25°C. The aqueous mixtures ([polymer] = 1 mg/m) were sonicated for 15 min and then filtrated with poly(tetrafluoroethylene) membrane filters (pore size: 0.45 μm) before measurements. The aqueous mixtures were kept at 25°C for about 24 h and then injected into the SEC-MALLS system using a 100 mM NaCl aqueous solution as an eluent. The apparent size of the copolymers and their micelles in water was evaluated with their SEC curves (by refractive index detector) on the basis of poly(ethylene oxide) (PEO) standard calibration; the peak-top molecular weight in water was compared with that in DMF (good solvent). The absolute weight-average molecular weight (*M<sub>w,H<sub>2</sub>O</sub>*) of the copolymers and their micelles in water was also determined by the MALLS detector to estimate the aggregation number (*N<sub>agg</sub>*).

As shown in Figure 2A and Figure S4, **P1**, **P2**, and **P3** showed unimodal SEC curves in water. The SEC curves in water shifted to molecular weight higher than corresponding counterparts in DMF. This indicates that the random copolymers induce intermolecular self-assembly to form multichain micelles in water. Similarly, **P1-M**, **P2-M**, and **P3-M** showed SEC curves with a peak-top molecular weight larger than those in DMF (Figure 2B–D). **P1-M** and **P3-M** exhibited relatively narrow molecular weight distribution in water.

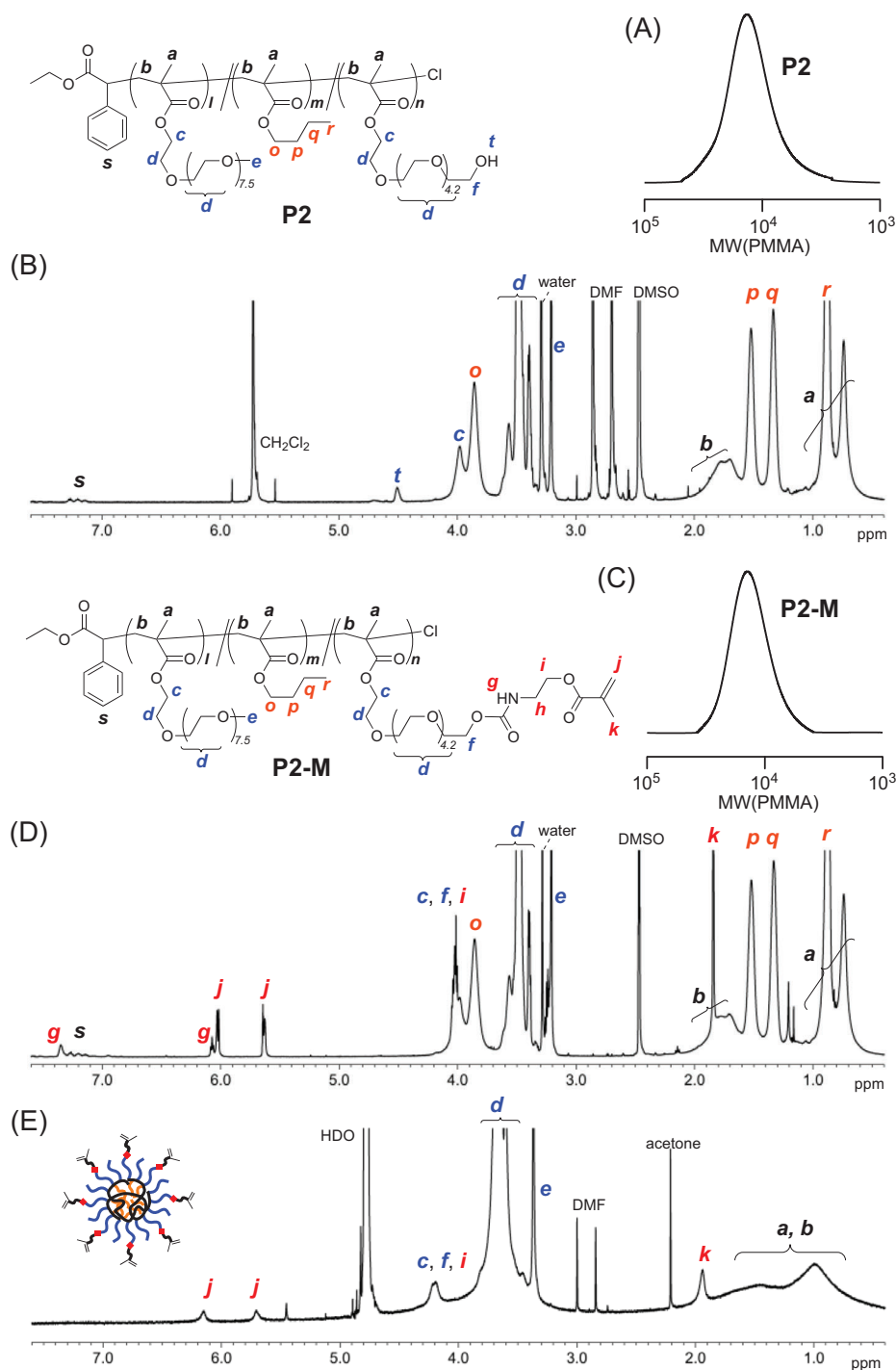


**FIGURE 1** (A, C) Size exclusion chromatography (SEC) curves (in DMF, 10 mM LiBr) and (B, D)  $^1\text{H}$  NMR spectra (in  $\text{DMSO-}d_6$  at  $25^\circ\text{C}$ ) of (A, B) **P2** and (C, D) **P2-M**. (E)  $^1\text{H}$  NMR spectra of **P2-M** in  $\text{D}_2\text{O}$  at  $25^\circ\text{C}$

$M_{w,\text{H}_2\text{O}}$  of **P1-M** and **P3-M** micelles in water were determined by MALLS to be 340,000 and 501,000, respectively. The  $M_{w,\text{H}_2\text{O}}$  values were close to those for corresponding **P1** and **P3** micelles in water. The aggregation number of **P1-M** and **P3-M** in water ( $N_{\text{agg}} = M_{w,\text{H}_2\text{O}}/M_{w,\text{DMF}}$ ) was calculated to be 9.6 and 8.9, respectively. The number of pendant methacrylate units per single micelle ( $n \times N_{\text{agg}}$ ) was estimated as 19 (**P1-M** micelle) and 36 (**P3-M** micelle). By tuning the DP and composition, we successfully controlled  $N_{\text{agg}}$  and the number of pendant methacrylate units of their micelles.

**P2-M** bearing 11 pendant methacrylate units exhibited an SEC curve containing shoulder or small peaks in a high molecular weight region in water (Figure 2C), indi-

cating that multichain micelles partly associated into larger aggregates.<sup>[34]</sup> This is because the methacrylate (MOI)-capped PEGs are more hydrophobic than other methyl ether PEGs (PEGMA). Considering that the apparent molecular weight of the **P2-M** micelle by SEC is larger than that of **P2** micelle with  $N_{\text{agg}}$  of 9, the **P2-M** micelle should have over  $10 N_{\text{agg}}$  and thereby over 100 pendant methacrylate units. The **P2-M** micelle was further analyzed by  $^1\text{H}$  NMR in  $\text{D}_2\text{O}$  (Figure 1E). The proton signals of the hydrophobic butyl groups and the polymethacrylate backbone turned broad, whereas those of the hydrophilic PEG chains and methacrylate units incorporated into the PEG terminals were clearly observed. This importantly supports that **P2-M** forms folded micelles via the association of hydrophobic butyl groups and

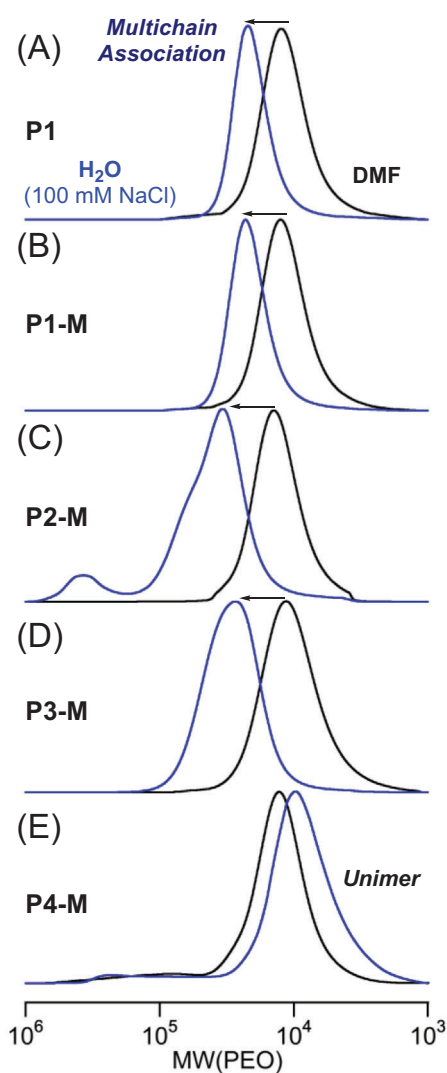


**FIGURE 2** Size exclusion chromatography (SEC) curves (with poly(ethylene oxide) [PEO] calibration) of (A) **P1**, (B) **P1-M**, (C) **P2-M**, (D) **P3-M**, and (E) **P4-M** in DMF (black) or H<sub>2</sub>O (100 mM NaCl) (blue)

the methacrylate units are located around the outer PEG shell layers in water.

In contrast, **P4** and **P4-M** without hydrophobic alkyl groups showed unimodal SEC curves in water and the peak-top molecular weight was close to that in DMF (Figure 2E and Figure S4).  $N_{agg}$  of **P4-M** was estimated to be 1.2 (Table 1), indicating that **P4-M** unimolecularly dissolves in H<sub>2</sub>O. The small peak shift of **P4-M** to lower molecular weight means the formation of a more compact structure in water than that in DMF due to the weak association of their pendant methacrylate units.

PEGMA/BMA (70 mol%) or DMA (50 mol%) random copolymer micelles are known to show lower critical solution temperature-type solubility in water and the cloud point (Cp) temperature of PEGMA/BMA (70 mol%) random copolymers is typically around 45°C.<sup>[31]</sup> This implies that radical crosslinking of their micelles should be conducted below the Cp temperature. Self-assembly and thermoresponsive properties of their copolymers into micelles may also be affected by hydrophilic monomers used for network polymer chains. Thus, we examined effects of temperature and hydrophilic monomers (used for network chains) on their random copolymer micelles in water by the Cp measurements of the micelle

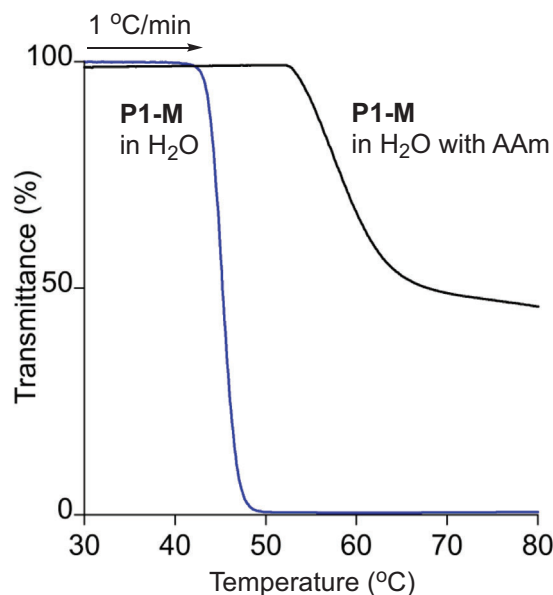


**FIGURE 3** Cloud point measurements of **P1-M** (1 mg/mL) in pure H<sub>2</sub>O (blue) or a 100 mg/mL AAm aqueous solution (black). The transmittance of the aqueous solutions was monitored at 670 nm upon heating from 25°C to 80°C

solutions (Figure 3 and Figure S5). Cp was defined as a temperature, at which the transmittance of the solutions turns to be 90%. Cp temperatures of the aqueous solutions of **P1-M**, **P2-M**, **P3-M**, and **P4-M** (1 mg/mL) were 45°C, 40°C, 60°C, and 65°C, respectively. The aqueous solution of **P1-M** containing AAm (100 mg/mL), a potential monomer for gel network chains, showed higher Cp at 55°C than the pure water solution of **P1-M** (Figure 3). The size distribution of **P1-M** micelles in water was evaluated by dynamic light scattering (Figure S6). The aqueous solution of a **P1-M** micelle (30 mg/mL, a typical concentration in gelation) showed bimodal size distribution in the presence of PEG methyl ether acrylate (PEGA) at 25°C or in the presence of AAm at 25°C or 45°C, whereas small objects with about 10–20 nm diameter were mainly formed. Importantly, the copolymer still maintained small micelles even in the presence of their hydrophilic monomers in water up to 45°C without decomposition of their self-assemblies into unimers. Therefore, we found that **P1-M–P3-M** micelles were available as crosslinking domains in water by applying appropriate temperatures between 25°C and 45°C in hydrogel preparation.

### 2.3 | Preparation and structure analysis of micelle-crosslinked hydrogels

Hydrogels were synthesized by FRP of hydrophilic monomers in the presence of **P1-M–P3-M** micelles or **P4-M** with ammonium persulfate (APS) and/or *N,N,N',N'*-tetramethylethylenediamine (TMEDA) at 25°C or 45°C for 1 h (Table 2). Various monomers were utilized to design hydrophilic networks of hydrogels: PEGA, 2-hydroxyethyl acrylate (HEA), AAm, 2-hydroxyethyl acrylamide (HEAAm), *N*-isopropylacrylamide (NIPAM), and *N,N*-dimethylacrylamide (DMAAm). The monomer concentration was set to 100 mg/mL. The concentration of **P1-M–P4-M** varied between 3 and 30 mg/mL, where the olefin concentration was also changed. Typically, Gel

TABLE 2 Synthesis of hydrogels via free radical polymerization (FRP) of hydrophilic monomers with P1-M–P4-M

Hydrogel <sup>a</sup>	Monomer	Crosslinker	Initiator	Temp. (°C)	[Crosslinker] (mg/mL)	[Monomer]/[Methacrylate pendants of crosslinkers] (mM)	$G^b$ (Pa)	$G''^b$ (Pa)
Gel 1	PEGA	P1-M	APS/TMEDA	25	30	210/2.4	198	8.06
Gel 2	PEGA	P2-M	APS/TMEDA	25	30	210/12	188	13.2
Gel 3	PEGA	P2-M	APS/TMEDA	25	5.5	210/2.2	9.19	4.14
Gel 4	AAM	P1-M	APS	45	30	1,400/2.4	1,010	205
Gel 5	AAM	P3-M	APS	45	30	1,400/2.8	727	133
Gel 6	AAM	P4-M	APS	45	3.0	1,400/2.3	495	168
Gel 7	DMAAm	P1-M	APS	45	30	1,000/2.4	520	102
Gel 8	HEA	P1-M	APS/TMEDA	25	30	860/2.4	581	35.2
Gel 9	AAM	P1-M	APS/TMEDA	25	30	1,400/2.4	797	202
Gel 10	HEAAm	P1-M	APS/TMEDA	25	30	870/2.4	835	108
Gel 11	NIPAAm	P1-M	APS/TMEDA	25	30	880/2.4	736	75.1
Gel 12	DMAAm	P1-M	APS/TMEDA	25	30	1,000/2.4	1,150	70.1

<sup>a</sup>Gel 1–Gel 12 were synthesized by free radical polymerization of hydrophilic monomers [poly(ethylene glycol) methyl ether acrylate (PEGA), 2-hydroxyethyl acrylate (HEA), acrylamide (AAM), *N,N*-dimethylacrylamide (DMAAm), 2-hydroxyethyl acrylamide (HEAAm), *N*-isopropyl acrylamide (NIPAAm)] in the presence of P1-M–P4-M crosslinkers with ammonium persulfate (APS) at 45°C or with APS and *N,N,N',N'*-tetramethylethylenediamine (TMEDA) at 25°C for 1 h: [hydrophilic monomer]<sub>0</sub>/[APS]<sub>0</sub>/[TMEDA]<sub>0</sub> = 100/1/0 or 2 (molar ratio).

<sup>b</sup>Storage modulus ( $G'$ ) and loss modulus ( $G''$ ) at a strain of 1% and a frequency of 1 Hz.

**1** was obtained from FRP of PEGA with a P1-M micelle (30 mg/mL), APS, and TMEDA in water at 25°C. Gel 4 was obtained from FRP of AAM with a P1-M micelle (30 mg/mL) and APS without TMEDA in water at 45°C. Both conditions (temperature and initiating systems) efficiently gave hydrogels.

To analyze the consumption of hydrophilic monomers and the formation of network chains in their hydrogels, we conducted in-situ <sup>1</sup>H NMR measurements of gelation for PEGA/P1-M micelle with APS/TMEDA in D<sub>2</sub>O at 25°C or AAM/P1-M micelle with APS in D<sub>2</sub>O at 45°C in NMR tubes (Figure 4). The mixture of PEGA/P1-M micelle in D<sub>2</sub>O (before crosslinking, Figure 4A) showed proton signals originating from the monomer and P1-M. After 1 h, the proton signals of both PEGA acrylate units (*A*, *B*) and the P1-M pendant methacrylate (*j*) disappeared completely (conversion: ~100%) and in turn, the proton signals of polyacrylate backbones (*A'*, *B'*) appeared (Figure 4B). The proton signals of the polymethacrylate backbones/butyl pendants of the P1-M micelle turned to hardly detected. These results support that poly(PEGA) network chains are formed and crosslinked with the P1-M micelle domains. Similarly, on the AAM/P1-M micelle hydrogel, the proton signals of AAM units (*F*, *H*) dramatically decreased in 1 h (conversion: ~99%), and those of polyacrylamide backbones (*F'*, *H'*) appeared (Figure 4C,D). Broad proton signals originating from the PEG chains of the P1-M micelle were still observed. We confirmed that the gelation of their hydrophilic monomers and P1-M micelles efficiently proceeded both with APS/TMEDA at 25°C and with APS at 45°C.

The internal structures of the AAM/P1-M micelle hydrogel in D<sub>2</sub>O were analyzed by small-angle neutron scattering (SANS) (Figure 5A). The P1-M micelle showed a scattering profile originating from the globular structure in D<sub>2</sub>O, and the radius of gyration ( $R_g$ ) was estimated to be 5 nm by the Guinier plot of the profile (Figure S7). The scattering profile of the hydrogel almost overlapped that of the P1-M micelle in the high- $q$  region (approximately 0.6–2 nm<sup>-1</sup>). This demon-

strates that the hydrogel consists of polyAAM network chains crosslinked with P1-M micelles. In addition, the scattering intensity of hydrogel around  $q < 0.1$  nm<sup>-1</sup> increased with decreasing  $q$ , reflecting the spatial inhomogeneity of the network structure.<sup>[36]</sup>

To clarify the structure of the micelles and hydrogel in detail, we carried out model fitting (Figure 5B and Supporting Information). First, we utilized a fitting model representing the core-shell spherical structure of the micelles. In this model, called the separate micelle model, a micelle is composed of a spherical BMA core with radius  $R_c$  and a shell with thickness  $t_s$  formed by PEGMA (volume fraction:  $\phi_s$ ) and D<sub>2</sub>O (volume fraction:  $1 - \phi_s$ ). Therefore, the overall radius of the micelle is  $R_s = R_c + t_s$ . We assumed the Gaussian distribution of  $R_c$ , taking the size distribution of micelles into account. The results of the fitting are given in Figure 5A (blue line) and Table 3. The scattering function well represented the entire scattering profile of the P1-M micelle solution and the high- $q$  region of the hydrogel profile, indicating that the compact structure of micelles ( $R_s \sim 5$  nm) was preserved in the hydrogel. In addition, the volume fraction of D<sub>2</sub>O in the micelle shells was large ( $1 - \phi_s = 0.77$ ). This means that the PEG chains in the shells were highly hydrated. The experimental datapoints of the hydrogel in the middle- $q$  and low- $q$  regions, however, did not agree with the theoretical scattering function of the separate micelles. This is probably because multiple micelles were interconnected by polyAAM chains.

To address the effects of interconnected adjacent two micelles, which is thought to be the dominating factor in causing the abovementioned deviation, we used another model (micelle pair model).<sup>[37]</sup> In this model, we suppose a pair of micelles with the abovementioned core-shell structure, whose surface-to-surface distance is  $l_{\text{pair}}$  and obeys Gaussian distribution. The best fit to the experimental data is shown in Figure 5A (red line) and Table 3. The experimental data points almost agreed with the theoretical curve, but the former slightly diverged from the latter, presumably due to the inhomogeneity of network structure and

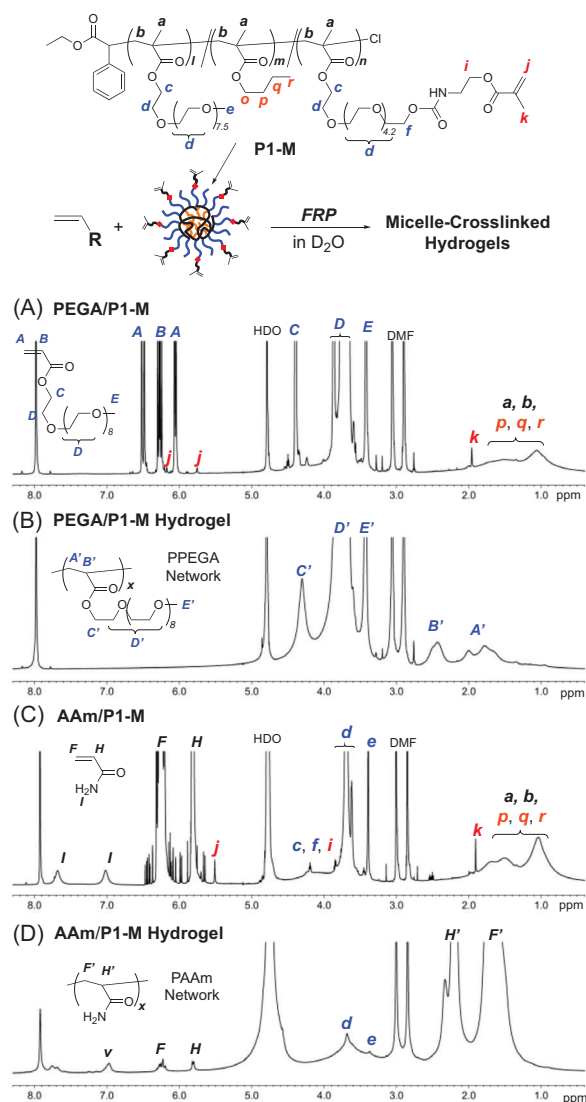


**FIGURE 4**  $^1\text{H}$  NMR spectra of (A) PEGA/P1-M (100/30 mg/mL) mixture, (B) PEGA/P1-M hydrogel, (C) AAm/P1-M (100/30 mg/mL) mixture, and (D) AAm/P1-M hydrogel in  $\text{D}_2\text{O}$  at  $25^\circ\text{C}$ . (B) The PEGA/P1-M hydrogel, as well as **Gel 1** (Table 2), was prepared within the NMR tube by crosslinking (A) the PEGA/P1-M mixture with APS/TMEDA (2.1/4.2 mM) in  $\text{D}_2\text{O}$  at  $25^\circ\text{C}$  for 1 h. (D) The AAm/P1-M hydrogel, as well as **Gel 4** (Table 2), was prepared within the NMR tube by crosslinking (C) the AAm/P1-M mixture with APS (14.1 mM) in  $\text{D}_2\text{O}$  at  $45^\circ\text{C}$  for 1 h

scattering from the polyAAm bridge chains between the micelles.

## 2.4 | Rheological properties of hydrogels

We investigated the effects of (1) micelle concentration, (2) crosslinking temperature, (3) crosslinking domain structures, and (4) hydrophilic monomers on viscoelastic properties of resulting hydrogels (**Gel 1–Gel 12**) by changing their synthetic conditions (Table 2). The rheological properties of their hydrogels were evaluated by oscillatory strain or frequency sweep measurements.

### 2.4.1 | Effects of micelle concentration on PEGA hydrogels

We prepared **Gel 1–Gel 3** via FRP of PEGA (100 mg/mL) with P1-M or P2-M micelles and APS/TMEDA in water at

**TABLE 3** Structural parameters of P1-M micelle and hydrogel<sup>a</sup>

$R_c/\text{nm}^b$	$t_s/\text{nm}^c$	$\phi_s^d$	$l_{\text{pair}}/\text{nm}^e$
3.7	1.3	0.23	18.4

<sup>a</sup>Determined by the model fitting of the SANS profiles. Details of the fitting models are given in Supporting Information.

<sup>b</sup>Average radius of the core. The standard deviation was chosen to be  $\sigma_{R_c} = 0.3R_c$ .

<sup>c</sup>Thickness of the shell.

<sup>d</sup>Volume fraction of PEGMA in the shell.

<sup>e</sup>Surface-to-Surface distance of micelles. The standard deviation was chosen to be  $\sigma_{l_{\text{pair}}} = 0.3l_{\text{pair}}$ .

$25^\circ\text{C}$ . The P1-M and P2-M micelles have 19 and over 100 olefin units ( $n \times N_{\text{agg}}$ ) on average, respectively. **Gel 1** and **Gel 2** contain 30 mg/mL of a P1-M micelle and a P2-M micelle, respectively. In the feed conditions, the concentration of their micelle domains is relatively close in both gels but the total concentration of the pendant methacrylate units in **Gel 2** is larger than that in **Gel 1**. **Gel 3** consists of a small amount of P2-M micelle (5.5 mg/mL) but the concentration of the pendant methacrylate is close to that in **Gel 1**. Figure 6A shows the shear storage modulus ( $G'$ ) and loss modulus ( $G''$ ) for **Gel 1–Gel 3** from oscillatory strain sweep measurement at a frequency of 1 Hz at  $25^\circ\text{C}$ . Typically, at 1% strain,  $G'$  for **Gel 1** and **Gel 2** was almost identical ( $\sim 200$  Pa) and over ten times larger than  $G''$ . The linear viscoelastic region for **Gel 1** ( $\sim 100\%$  strain) was larger than that for **Gel 2** ( $\sim 20\%$  strain).  $G'$  for **Gel 3** was much smaller than that for **Gel 1** and **Gel 2** and only about twice larger than  $G''$ .  $G'$  and  $G''$  for **Gel 1–Gel 3** were evaluated by oscillatory frequency sweep measurements at 1% strain from  $10^{-1}$  to  $10^2$  rad/s at  $25^\circ\text{C}$  (Figure 6B). **Gel 1** and **Gel 2** showed almost constant  $G'$  in a wide range of frequency ( $10^{-1}$ – $10^2$  rad/s) and the  $G'$  values were larger than  $G''$  in the frequency region, indicative of the efficient gelation on **Gel 1** and **Gel 2**.

Taking these results into consideration, we found the following trends: (1)  $G'$  for their hydrogels depends on the concentration of micelle domains and is hardly affected by the local concentration of pendant methacrylates per a single micelle ( $n \times N_{\text{agg}}$ ) in the case of 30 mg/mL of their micelles. About 20 methacrylate units per micelle domain were enough to crosslink polyPEGA network chains if 30 mg/mL of micelles were used. (2) **Gel 2** was more brittle than **Gel 1**. This is because P2-M micelles with a large number of methacrylate units ( $>100$ ) contribute as chemical crosslinking in **Gel 2** more greatly than P1-M micelles in **Gel 1**; the reversible and physical crosslinking by P2-M micelles would be more restricted than those by P1-M micelles. It is also confirmed that poly(PEGA) network chains were not only physically but also covalently crosslinked with a P1-M micelle in **Gel 1** by the following experiment: **Gel 1** mostly collapsed in methanol but the insoluble aggregates and microgels partly remained (Figure S8).

### 2.4.2 | Effects of crosslinking conditions and micelle domains on AAm hydrogels

To evaluate the effects of the crosslinking conditions on the rheological properties, we prepared AAm hydrogels using a P1-M micelle crosslinker in water by the following condi-

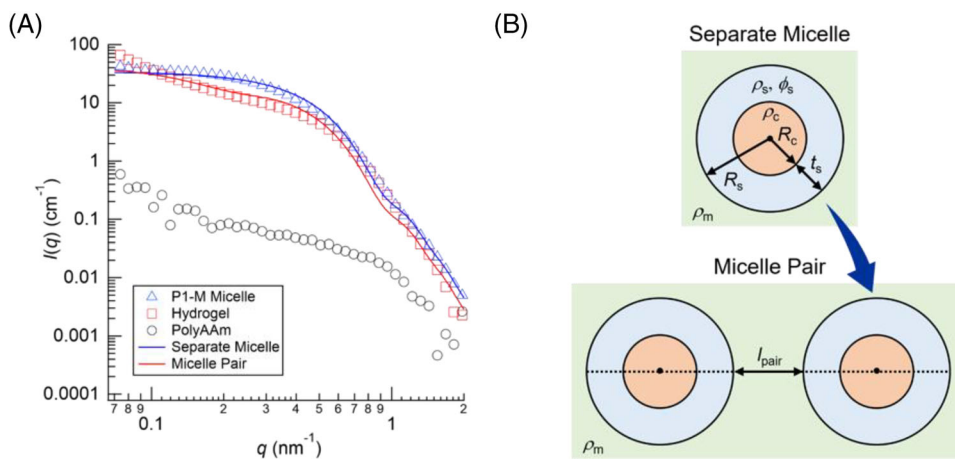


**FIGURE 5** Small-angle neutron scattering (SANS) analysis of **P1-M** micelle and hydrogel: (A) SANS profiles of acrylamide (AAm)/**P1-M** hydrogel, and polyAAm ( $M_n = 69,100$ ,  $M_w/M_n = 1.97$  by size exclusion chromatography [SEC] with poly(ethylene oxide) [PEO] calibration) in  $D_2O$  at  $25^\circ C$  (open symbols) and scattering functions by the separate micelle (blue line) and micelle pair (red line) models, and (B) schematic representations of the models. [**P1-M** micelle] = 30 mg/mL, [hydrogel] = 130 mg/mL, and [polyAAm] = 100 mg/mL

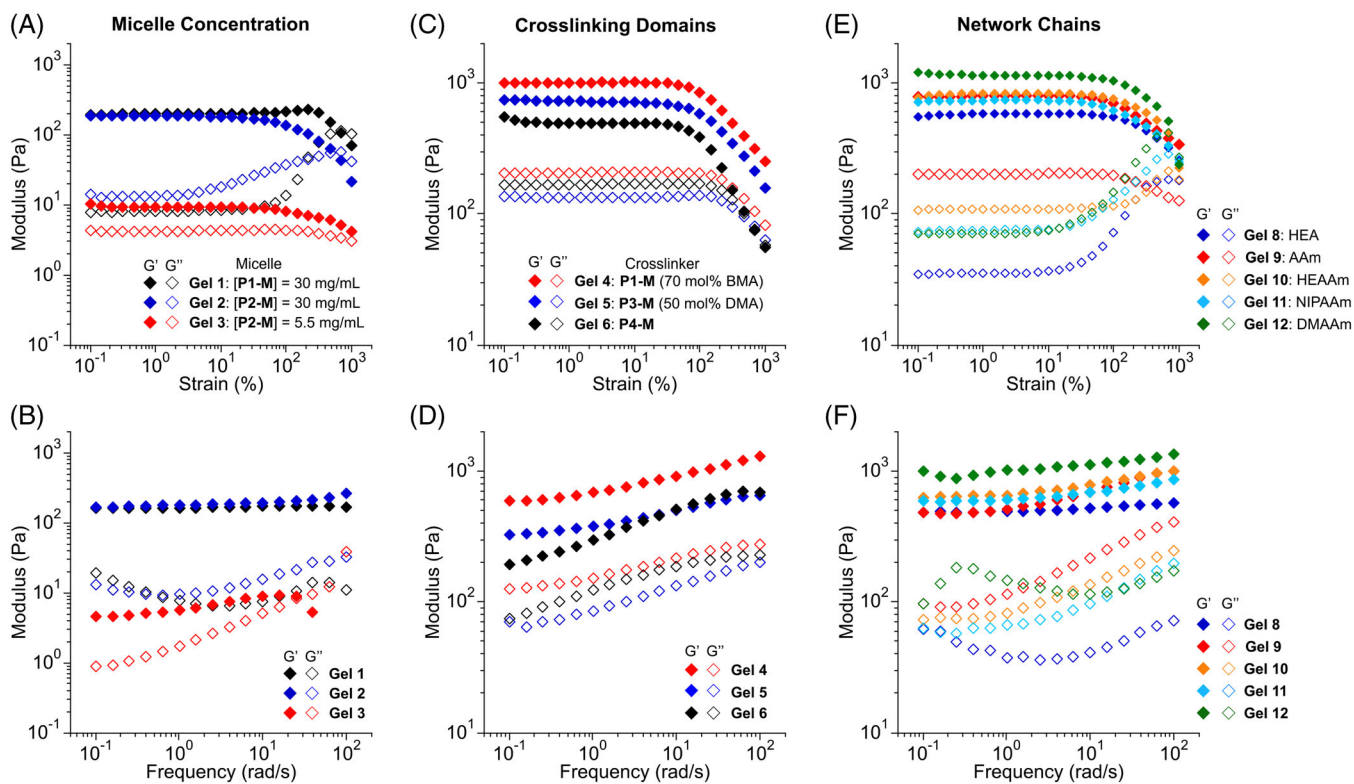
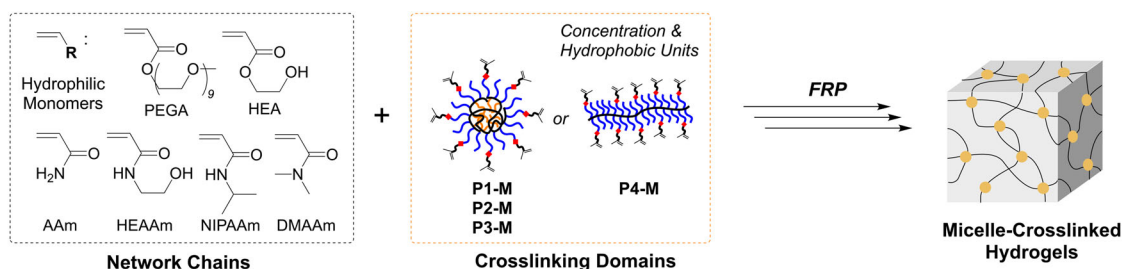


**FIGURE 6** (A, C, E) Oscillatory strain sweep measurements of hydrogels (A: **Gel 1–Gel 3**, C: **Gel 4–Gel 6**, E: **Gel 8–Gel 12**) at a frequency ( $\omega$ ) of 1 Hz at  $25^\circ C$ . (B, D, F) Oscillatory frequency sweep measurements of hydrogels (B: **Gel 1–Gel 3**, D: **Gel 4–Gel 6**, F: **Gel 8–Gel 12**) at 1% strain ( $\gamma$ ) from  $10^{-1}$  to  $10^2$  rad/s at  $25^\circ C$ . Shear storage modulus ( $G'$ ,  $\blacklozenge$ ) and loss modulus ( $G''$ ,  $\diamond$ )

tions: with APS at 45°C (**Gel 4**), with APS/TMEDA at 25°C (**Gel 9**), and with APS at 25°C (Table 2 and Figure S9).  $G'$  and  $G''$  for the three hydrogels were evaluated by oscillatory strain sweep measurement at a frequency of 1 Hz at 25°C (Figure 6C,E and Figure S9). All the hydrogels showed the linear viscoelastic region of  $G'$  up to about 50% strain;  $G'$  was 5–10 times larger than  $G''$  at 1% strain. The  $G'$  values depended on the crosslinking conditions: 1,010 Pa (with APS at 45°C, **Gel 4**), 797 Pa (with APS/TMEDA at 25°C, **Gel 9**), 267 Pa (with APS at 25°C). The difference of  $G'$  is probably related to the length of polyAAm network chains and/or crosslinking efficiency dependent on their reaction conditions.

A **P3-M** micelle with 50 mol% DMA, as well as a **P1-M** micelle with 70 mol% DMA, potentially serves as covalently and physically crosslinking units though **P4-M** works only as covalent crosslinking units. To evaluate the effects of the hydrophobic units on the physical properties, we synthesized AAm hydrogels (**Gel 5** or **Gel 6**) by FRP of AAm with a **P3-M** micelle (30 mg/mL) or **P4-M** (3.0 mg/mL) with APS at 45°C. **Gel 5** (with a **P3-M** micelle) and **Gel 6** (with **P4-M**), as well as **Gel 4** (with a **P1-M** micelle), showed linear viscoelastic region up to 40%–100% strain on strain sweep measurement, and their  $G'$  values were much larger than corresponding  $G''$  values (Figure 6C).  $G'$  values at 1% strain increased as follows: 1,010 Pa (**Gel 4**), 727 Pa (**Gel 5**), and 495 Pa (**Gel 6**). The number density of the **P1-M** micelle (0.088 mM) is larger than that of the **P3-M** micelle (0.060 mM) or the **P4-M** (0.057 mM), although the concentration of pendant methacrylate units (2.3–2.8 mM) is almost constant in the three gels. Therefore, the trend of  $G'$  would be related to the number density of crosslinking domains. Effects of physical crosslinking by the association of their hydrophobic groups were more remarkably observed in stress relaxation experiments as described later.

### 2.4.3 | Design of hydrophilic polymer networks

We further prepared hydrogels (**Gel 8–Gel 12**) consisting of various hydrophilic polymer networks by FRP of HEA, AAm, HEAAm, NIPAM, and DMAAm as hydrophilic monomers with a **P1-M** micelle and APS/TMEDA at 25°C. All the hydrogels showed the linear viscoelastic region of  $G'$  up to around 100% strain in oscillatory strain sweep measurement at a frequency of 1 Hz at 25°C (Figure 6E).  $G'$  and  $G''$  for the hydrogels were also evaluated by oscillatory frequency sweep measurements at 1% strain from  $10^{-1}$  to  $10^2$  rad/s at 25°C (Figure 6F). For example, **Gel 8** with polyHEA networks showed almost constant  $G'$  in a wide range of frequency ( $10^{-1}$ – $10^2$  rad/s) and the  $G'$  values were larger than  $G''$  in the frequency region. As demonstrated here, we successfully developed versatile synthetic systems of micelle-crosslinked hydrogels via FRP of hydrophilic monomers in the presence of olefin-bearing micelles in water.

## 2.5 | Tensile and stress relaxation behavior of hydrogels

PEGMA-based random copolymer micelles induce chain exchange in the water around room temperature.<sup>[32,35]</sup> The exchange kinetics depend on the hydrophobic monomer units consisting of the micelle cores: The chain exchange of PEGMA/BMA random copolymer micelles is faster than that of PEGMA/DMA random copolymer micelles at 25°C. Thus, crosslinking domains of random copolymer micelles are also expected to show chain exchange within hydrogels.<sup>[32]</sup> To investigate the effects of such chain exchange on the mechanical properties of hydrogels, tensile tests and stress relaxation measurements were conducted for **Gel 4**, **Gel 5**, and **Gel 6**. All the hydrogels showed highly stretchable properties (Figure 7A). **Gel 4** consisting of **P1-M** micelles was more stretchable up to over 1,000% than **Gel 5** consisting of **P3-M** micelles. The stretchable properties of **Gel 4** most likely arise from the efficient chain exchange of PEGMA/BMA-based **P1-M** micelles within the network structures: The micelle-crosslinking domains can reversibly be regenerated within the hydrogel networks even though the random copolymer chains are once pulled out from the micelle domains during the elongation process of the hydrogel. We can also stretch **Gel 4** to over 1,000% strain by hand without breaking (Figure 7B). **Gel 6** consisting of covalent crosslinking with **P4-M** was also well stretched. This is probably due to the concentration of **P4-M** (3 mg/mL) lower than the other micelle crosslinking domains (**P1-M** and **P3-M**, 30 mg/mL). The breaking strain of **Gel 4** was close to that of **Gel 6**.

The chain exchange behavior of micelle-crosslinking domains was examined by shear stress relaxation measurements of **Gel 4**, **Gel 5**, and **Gel 6** at 5, 25, and 40°C, where the strain was kept at 10% (Figure 7C–E). The shear stress of **Gel 4** gradually decreased with time progress and the stress relaxation was promoted by increasing temperature. Similarly, **Gel 5** also showed stress relaxation at 40°C, whereas the decay of the stress was slower than that for **Gel 4** at 40°C. In contrast, **Gel 6** only showed a small decrease in the stress and the trend was almost independent of the temperature. **Gel 4** and **Gel 5** showed quite slow decay of the stress at 5°C at almost the same speed as that for **Gel 6**. These results indicate the followings: (1) The stress relaxation on **Gel 4** and **Gel 5** originates from the chain exchange of micelle-crosslinking domains. The chain exchange within their hydrogel networks, as well as that of corresponding random copolymer micelles in water,<sup>[32]</sup> is accelerated upon heating. (2) The chain exchange of PEGMA/BMA random copolymer micelles in **Gel 4** is faster than that of PEGMA/DMA counterparts in **Gel 5**. PEGMA/DMA random copolymer chains were hardly exchanged at 25°C. (3) Micelle-crosslinking domains within **Gel 4** and **Gel 5** are “frozen” at 5°C without chain exchange like covalently crosslinked domains in **Gel 6**. The slow decay of the stress for **Gel 4** and **Gel 5** at 5°C, as well as that for **Gel 6**, is probably due to the relaxation of their entangled polyAAm network chains.

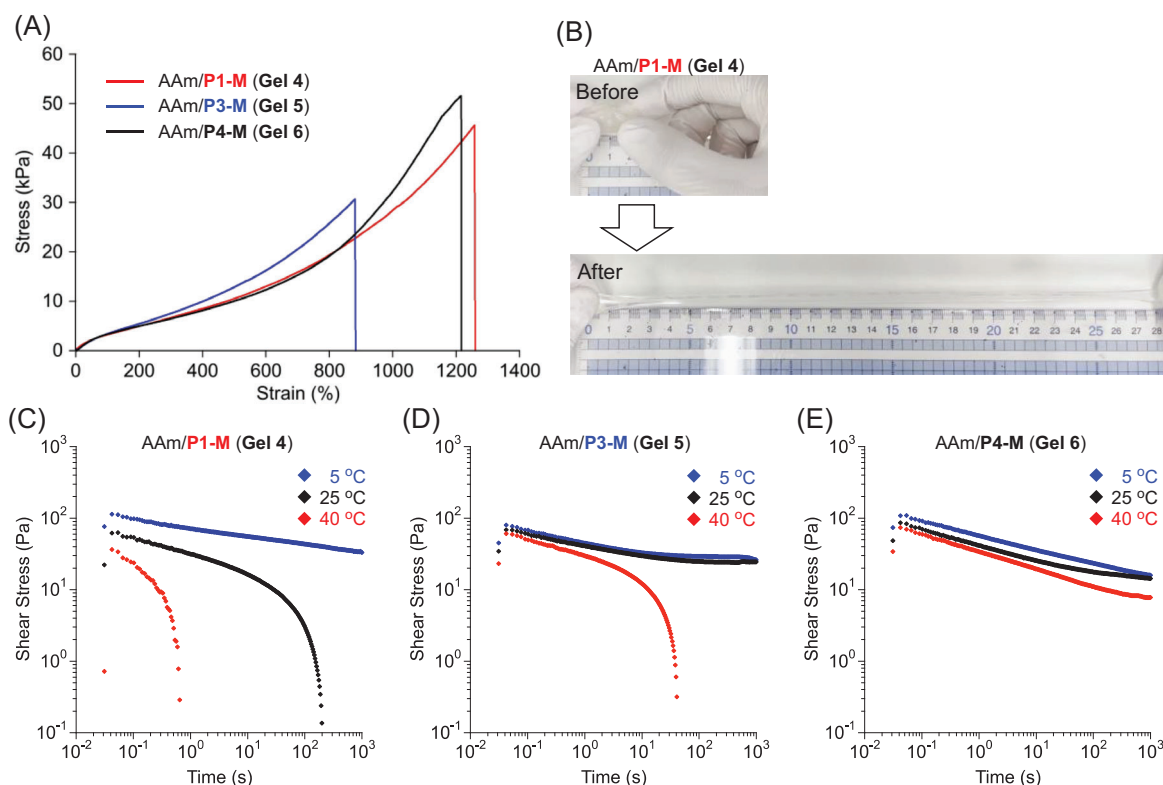


**FIGURE 7** (A) Tensile stress-strain curve of an acrylamide (AAm)/P1-M micelle hydrogel (Gel 4, red), an AAm/P3-M micelle hydrogel (Gel 5, blue), and an AAm/P4-M hydrogel (Gel 6, black). (B) Photographs of an elongated Gel 4. Stress relaxation measurement of (C) Gel 4, (D) Gel 5, and (E) Gel 6 at 5°C (blue), 25°C (black), and 40°C (red)

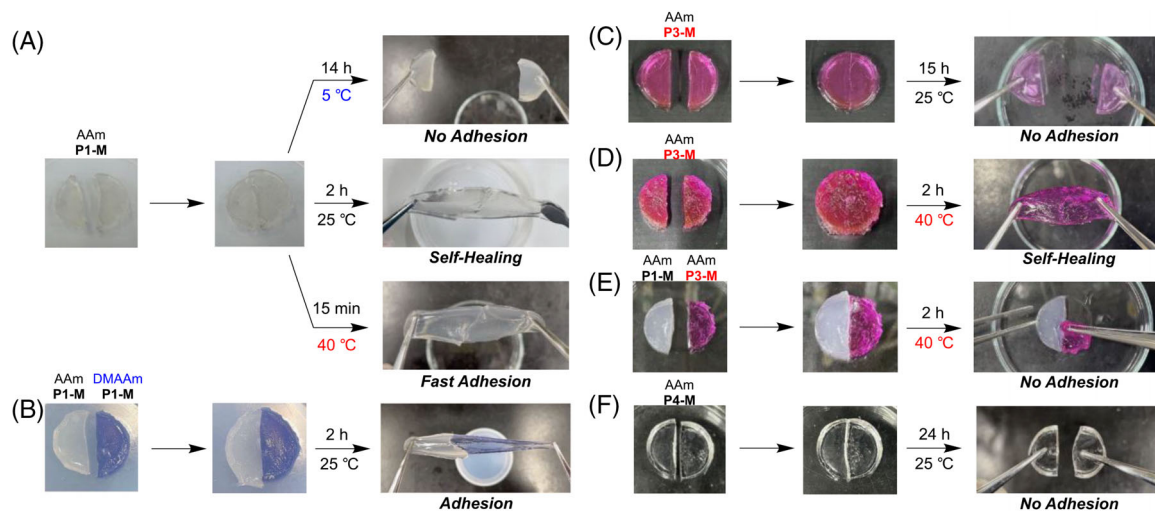


**FIGURE 8** Self-healing and self-adhesive properties of hydrogels. (A) Effects of temperature (5, 25, and 40°C) on the self-healing properties of Gel 4 (AAm/P1-M hydrogel). Adhesive properties of (B) Gel 4 and Gel 7 (DMAAm/P1-M hydrogel) at 25°C, (C, D) Gel 5 (AAm/P3-M hydrogel) at (C) 25°C or (D) 40°C, (E) Gel 4 and Gel 5 at 40°C, and (F) Gel 6 (AAm/P4-M hydrogel) at 25°C

## 2.6 | Self-healing and adhesive properties of hydrogels

Focusing on the chain exchange of random copolymer micelles, we examined the self-healing and adhesive properties of hydrogels. First, Gel 4 crosslinked with P1-M micelles was cut into two pieces and the cut gels were again contacted at 5°C, 25°C, and 40°C (Figure 8A). The cut gels adhered at 25°C for at least 2 h or at 40°C for 15 min, whereas the gels were not adhesive at 5°C at all. The self-healing

properties are derived from the chain exchange between micelle domains on the gel surfaces; the fast adhesion at 40°C is due to the fast chain exchange upon heating. Gel 5 crosslinked with P3-M micelles adhered at 40°C in 2 h (Figure 8D), whereas Gel 5 was hardly adhesive at 25°C in 15 h (Figure 8C). This is due to the quite slow exchange of PEGMA/DMA copolymer chains at 25°C. The adhesion of cut Gel 5 at 40°C was weaker than that of cut Gel 4 at 25°C. This suggests that P3-M micelles contain relatively large amounts of pendant methacrylates to contribute more as

covalent crosslinking units. Those healing and adhesive properties were consistent with the trend of the stress-relaxation of **Gel 4** and **Gel 5**. **Gel 6** crosslinked covalently with **P4-M** was never adhesive at all (Figure 8F).

Interestingly, **Gel 4** (AAM/**P1-M**) adhered to **Gel 9** (DMAAm/**P1-M**) at 25°C in 2 h although the network polymer chains of their hydrogels were different (Figure 8B). This means that hydrogels consisting of identical random copolymer micelles as crosslinking domains are adhesive, independent of the structures of network polymers. In contrast, **Gel 4** containing **P1-M** micelles with BMA units never adhered to **Gel 5** containing **P3-M** micelles with DMA units at 40°C in 2 h (Figure 8E) although **Gel 5** was adhesive each other at 40°C in 2 h (Figure 8D). These results indicate that their micelle-crosslinking domains exhibit self-sorting (selective self-assembly) behavior on their gel surfaces. Such selective adhesion properties are one of the characteristics of hydrogels consisting of random copolymer micelles as crosslinked domains.

Finally, a tensile test of the self-healed **Gel 4** was conducted (Figure S11). The sample was prepared by the adhesion of two cut gel pieces at 25°C for 2 h. The connected gel stretched up to about 80% strain and then fractured at the adhesion point, although the original **Gel 4** was stretched around 1,000%. This is because the broken covalent bonds of multiple polyAAM network chains are not repaired and the tensile stress is concentrated on micelle-crosslinking domains regenerated at the adhesion interface of the cut gels.<sup>[38]</sup> The cut and re-connecting method, examined herein, would be useful to produce hydrogels with controlled breaking points by introducing the relatively weak adhesion interface into the desired sites.

### 3 | CONCLUSION

In summary, we established versatile synthetic systems of highly stretchable, self-healing, and selectively adhesive hydrogels via FRP of hydrophilic vinyl monomers coupled with methacrylate-bearing random copolymer micelles. The random copolymer micelles efficiently served as physical and covalent crosslinking domains for hydrogels. Thus, the physical properties of hydrogels were controlled by designing the micelles as crosslinked domains. The self-healing and adhesive properties and their kinetics depended on the chain exchange and selective association (self-sorting) of the micelles. This system further affords the versatile design of network polymer chains. Therefore, the synthetic strategy of micelle-crosslinked hydrogels, developed herein, opened a new possibility to produce hydrogels with stretchable, self-healing, and selectively adhesive properties as desired and would bring innovation in various research fields for applications such as selectively adhesive biomaterials.

### ACKNOWLEDGMENTS

This work was supported by Japan Society for the Promotion of Science KAKENHI Grants (JP19K22218, JP20H02787, JP20H05219, and JP22H04539), by The Ogasawara Foundation for the Promotion of Science & Engineering, by The Noguchi Institute, and by Iketani Science and Technology Foundation. SANS was performed on BL15 at the Materials and Life Science Experimental Facility (MLF) of the Japan Proton Accelerator Research Complex (J-PARC) (Proposal

No. 2022A0028). H.A. thanks Iwadare Scholarship Foundation for the scholarship. The authors acknowledge the support of the Quantum Beam Analyses Alliance (QBAA).

### CONFLICT OF INTEREST

The authors declare no conflict of interest.

### DATA AVAILABILITY STATEMENT

The data that support the findings of this study are available from the corresponding author upon reasonable request.

### ORCID

Motoki Shibata  <https://orcid.org/0000-0003-1771-4248>

Mikihito Takenaka  <https://orcid.org/0000-0002-6803-048X>

Makoto Ouchi  <https://orcid.org/0000-0003-4540-7827>

Takaya Terashima  <https://orcid.org/0000-0002-9917-8049>

### REFERENCES

1. K. Y. Lee, D. J. Mooney, *Chem. Rev.* **2001**, *101*, 1869.
2. T. R. Hoare, D. S. Kohane, *Polymer* **2008**, *49*, 1993.
3. S. Van Vlierbergh, P. Dubruel, E. Schacht, *Biomacromolecules* **2011**, *12*, 1387.
4. X. Du, J. Zhou, J. Shi, B. Xu, *Chem. Rev.* **2015**, *115*, 13165.
5. B. Wang, W. Xu, Z. Yang, Y. Wu, F. Pi, *Macromol. Rapid Commun.* **2022**, *43*, 2100785.
6. R. Ikura, J. Park, M. Osaki, H. Yamaguchi, A. Harada, Y. Takashima, *NPG Asia Mater.* **2022**, *14*, 10.
7. Y. Kashiwagi, T. Katashima, M. Nakahata, Y. Takashima, A. Harada, T. Inoue, *J. Polym. Sci. Part B Polym. Phys.* **2018**, *56*, 1109.
8. T. Katashima, *Polym. J.* **2021**, *53*, 1073.
9. J. P. Gong, Y. Katsuyama, T. Kurokawa, Y. Osada, *Adv. Mater.* **2003**, *15*, 1155.
10. J. P. Gong, *Soft Matter* **2010**, *6*, 2583.
11. K. Singh, A. Ohlan, P. Saini, S. K. Dhawan, *Polym. Adv. Technol.* **2008**, *19*, 647.
12. Y. Okumura, K. Ito, *Adv. Mater.* **2001**, *13*, 485.
13. K. Ito, *Polym. J.* **2007**, *39*, 489.
14. E. A. Appel, F. Biedermann, U. Rauwald, S. T. Jones, J. M. Zayed, O. A. Scherman, *J. Am. Chem. Soc.* **2010**, *132*, 14251.
15. A. Harada, R. Kobayashi, Y. Takashima, A. Hashidzume, H. Yamaguchi, *Nat. Chem.* **2011**, *3*, 34.
16. D. C. Tuncaboylu, M. Sari, W. Oppermann, O. Okay, *Macromolecules* **2011**, *44*, 4997.
17. J. Hao, R. A. Weiss, *Macromolecules* **2011**, *44*, 9390.
18. L. Li, R. Jiang, J. Chen, M. Wang, X. Ge, *RSC Adv.* **2017**, *7*, 1513.
19. S. Gu, G. Cheng, T. Yang, X. Ren, G. Gao, *Macromol. Mater. Eng.* **2017**, *302*, 1.
20. U. Gulyuz, *Macromol. Mater. Eng.* **2021**, *306*, 1.
21. Y. N. Sun, G. R. Gao, G. L. Du, Y. J. Cheng, J. Fu, *ACS Macro Lett.* **2014**, *3*, 496.
22. Y. Du, S. Jia, Y. Chen, L. Zhang, J. Tan, *ACS Macro Lett.* **2021**, *10*, 297.
23. Y. Liu, W. Zhou, Q. Zhou, K. Peng, A. Yasin, H. Yang, *RSC Adv.* **2017**, *7*, 29489.
24. Y. Sun, S. Lu, Q. Li, Y. Ren, Y. Ding, H. Wu, X. He, Y. Shang, *Eur. Polym. J.* **2020**, *133*, 109761.
25. Y. Li, D. Wang, J. Wen, J. Liu, D. Zhang, J. Li, H. Chu, *Adv. Funct. Mater.* **2021**, *31*, 1.
26. M. Tan, T. Zhao, H. Huang, M. Guo, *Polym. Chem.* **2013**, *4*, 5570.
27. T. Zhao, M. Tan, Y. Cui, C. Deng, H. Huang, M. Guo, *Polym. Chem.* **2014**, *5*, 4965.
28. L. Xiao, C. Liu, J. Zhu, D. J. Pochan, X. Jia, *Soft Matter* **2010**, *6*, 5293.
29. L. Xiao, J. Zhu, J. D. Londono, D. J. Pochan, X. Jia, *Soft Matter* **2012**, *8*, 10233.
30. Y. Hirai, T. Terashima, M. Takenaka, M. Sawamoto, *Macromolecules* **2016**, *49*, 5084.
31. S. Imai, Y. Hirai, C. Nagao, M. Sawamoto, T. Terashima, *Macromolecules* **2018**, *51*, 398.

32. S. Imai, M. Takenaka, M. Sawamoto, T. Terashima, *J. Am. Chem. Soc.* **2019**, *141*, 511.
33. Y. Kimura, M. Takenaka, M. Takenaka, M. Ouchi, T. Terashima, *Macromolecules* **2020**, *53*, 4942.
34. M. Shibata, T. Terashima, T. Koga, *Macromolecules* **2021**, *54*, 5241.
35. M. Hibino, K. Tanaka, M. Ouchi, T. Terashima, *Macromolecules* **2022**, *55*, 178.
36. C. Tsitsilianis, G. Serras, C. H. Ko, F. Jung, C. M. Papadakis, M. Rikkou-Kalourkoti, C. S. Patrickios, R. Schweins, C. Chassenieux, *Macromolecules* **2018**, *51*, 2169.
37. A. V. Dobrynin, M. Rubinstein, S. P. Obukhov, *Macromolecules* **1996**, *29*, 2974.
38. Z. Zhao, Y. Bai, J. Sun, K. Lv, S. Lei, J. Qiu, *J. Appl. Polym. Sci.* **2021**, *138*, 38.

## SUPPORTING INFORMATION

Additional supporting information can be found online in the Supporting Information section at the end of this article.

**How to cite this article:** H. Asai, M. Shibata, M. Takenaka, S. Takata, K. Hiroi, M. Ouchi, T. Terashima, *Aggregate* **2023**, *4*, e316.  
<https://doi.org/10.1002/agt2.316>